

Research Paper

The m⁶A demethylase ALKBH5 controls trophoblast invasion at the maternal-fetal interface by regulating the stability of *CYR61* mRNA

Xiao-Cui Li^{1, #}, Feng Jin^{2, #}, Bei-Ying Wang¹, Xiang-Jie Yin¹, Wei Hong¹, Fu-Ju Tian^{3,4}✉

1. Department of Obstetrics and Gynecology, Shanghai First Maternity and Infant Hospital, Tongji University School of Medicine, Shanghai 201204, P.R. China.
2. Department of Obstetrics and Gynecology, the Shanghai Jiaotong University Affiliated Sixth People's Hospital, Shanghai 200233, P.R. China.
3. The International Peace Maternity & Child Health Hospital, Shanghai Jiao Tong University School of Medicine, Shanghai 200030, P. R. China.
4. Clinical and Translational Research Center, Shanghai First Maternity and Infant Hospital, Tongji University School of Medicine, Shanghai, 200040, China.

These authors contributed equally to this work.

✉ Corresponding author: **Fu-Ju Tian**, Clinical and Translational Research Center, Shanghai First Maternity and Infant Hospital, Tongji University School of Medicine, Shanghai, 200040, China, and the International Peace Maternity & Child Health Hospital, Shanghai Jiao Tong University School of Medicine, Shanghai 200030, P. R. China. E-mail: fjtian@sibs.ac.cn© Ivyspring International Publisher. This is an open access article distributed under the terms of the Creative Commons Attribution (CC BY-NC) license (<https://creativecommons.org/licenses/by-nc/4.0/>). See <http://ivyspring.com/terms> for full terms and conditions.

Received: 2018.11.29; Accepted: 2019.04.09; Published: 2019.05.31

Abstract

N⁶-Methyladenosine (m⁶A) is the most prevalent internal modification in mammalian mRNAs. Although m⁶A is important in many biological processes, its roles in the placenta are unclear.

Methods: Levels of global mRNA m⁶A methylation and ALKBH5 expression in recurrent miscarriage (RM) patients were determined using quantitative reverse transcription-PCR (qRT-PCR), m⁶A RNA methylation quantification, and immunohistochemical methods. Using ALKBH5 overexpression and knockdown methods, we determined the role of ALKBH5 in trophoblast invasion at the maternal interface through trophoblasts and an extravillous explant culture experiments. Furthermore, the regulation of *CYR61* by ALKBH5 was explored by RNA-sequencing coupled with methylated RNA immunoprecipitation.

Results: We found that the level of global mRNA m⁶A methylation was significantly decreased in placental villous tissue from RM patients, while ALKBH5 expression was specifically unregulated. Furthermore, we demonstrated that ALKBH5 knockdown in human trophoblast promoted trophoblast invasion. Conversely, overexpression of ALKBH5 inhibited cell invasion. ALKBH5 knockdown promoted trophoblast invasion in villous explant culture experiments, while overexpression of ALKBH5 repressed these effects. Furthermore, we clarified that ALKBH5 inhibited trophoblast invasion by regulating *CYR61* mRNA stability, and this RNA regulation is m⁶A dependent. Mechanistic analyses showed that decreased ALKBH5 in trophoblast increased the half-life of *CYR61* mRNA and promoted steady-state *CYR61* mRNA expression levels.

Conclusions: We elucidated the functional roles of ALKBH5 and mRNA m⁶A methylation in trophoblast and identified a novel RNA regulatory mechanism, providing a basis for further exploration of broad RNA epigenetic regulatory patterns in RM diseases.

Key words: N6-methyladenosine; ALKBH5; *CYR61*; trophoblast invasion; recurrent miscarriage.

Introduction

Among the more than 100 types of post-transcriptional modifications identified in RNAs thus far, N⁶-methyladenosine (m⁶A) RNA methylation is the most abundant internal mRNA

modification [1]. This modification is present transcriptome-wide in at least one-fourth of all RNAs, accounting for approximately 50% of the total methylated ribonucleotides and 0.1-0.4% of all

adenosines in total cellular RNAs [2]. m⁶A RNA methylation is a reversible nucleotide modification detected in at least 20% of mouse and human cellular mRNAs in diverse cell types [3] and is typically located in a consensus motif RRACH (R = A or G; methylated adenosine residue is underscored) and enriched near the translation termination codon in 3'-untranslated regions (3'-UTRs) [4-6]. In addition, previous study indicates that m⁶A modification has been most strongly linked to increased mRNA degradation [7]. In mammal, m⁶A is deposited cotranscriptionally by a methyltransferase complex consisting of METTL3, METTL14, WTAP, KIAA1429, and RBM15/RBM15B [8-10]. In turn, it can be removed by two m⁶A demethylases, fat mass and obesity-associated protein (FTO) and AlkB homolog 5 (ALKBH5) [11-13]. Recently, a relationship between FTO and obesity was established in animal research. Study found that FTO regulates adipogenesis and energy homeostasis, and FTO overexpression results in increased food intake and obesity in mice. While FTO deficiency protected against obesity [14, 15]. By contrast, ALKBH5 is localized in the nucleus, which is most highly expressed in the testes but has low expression in the heart and brain, and the m⁶A mRNA level significantly decreased in ALKBH5-overexpressing cells [16]. ALKBH5 strictly selects a substrate in catalytic progression, and the loss of ALKBH5 impairs RNA metabolism, mRNA export and assembly [16]. Interestingly, ALKBH5 has been shown to be involved in glioblastoma and breast cancer stem cell [17, 18]. In addition, ALKBH5 has been reported to play a key role in spermatogenesis. Male mice ALKBH5 knockout are completely infertile due to severe germ cell apoptosis and affects meiotic metaphase-stage spermatocytes [16, 19]. Thus, these studies clearly indicate that changes in the expression of key genes, which are sensitive to the function of m⁶A modulator, can cause significant phenotype changes. However, to date, very few studies have focused on how ALKBH5 is dysregulated in the pathogenesis of recurrent miscarriage (RM).

Cysteine-rich angiogenic inducer 61 (CYR61), a matricellular protein, is a member of the CCN family of secreted matricellular proteins that includes connective tissue growth factor (CCN2), NOV (CCN3), WISP-1 (CCN4), WISP-2 (CCN5), and WISP-3 (CCN6) [20]. This protein consists of 4 conserved domains: insulin-like growth factor-binding protein (IGFBP), von Willebrand factor type C repeat (VWC), thrombospondin type 1 (TSP-1) repeat and a carboxyl-terminal (CT) domain containing a cysteine knot motif. CYR61 was originally shown to act as a growth factor-inducible immediate-early gene, present in serum and

platelet-derived growth factor-stimulated mouse BALB/c 3T3 cells [21]. The biological properties of CYR61 in the regulation of cell survival, proliferation, differentiation, migration, adhesion and synthesis of ECM have been demonstrated to be important in the progression of embryogenesis [22]. In the human placenta, CYR61 is expressed in endothelial cells of placental vessels, stromal cells, and interstitial extravillous trophoblast (EVT) giant cells, and the expression levels increase during pregnancy [23]. Kipkeew *et al.* reported that CYR61 could enhance the migratory capability of SGHPL-5 trophoblast cells through the activation of the FAK signaling pathway [24]. Moreover, clinical evidence has also shown the downregulation of CYR61 in the placenta in women with preeclampsia compared with normal matched controls [25]. These studies indicate that the dysfunctional expression of CYR61 might be responsible for the impaired trophoblast cell invasion in pregnancy-associated diseases.

Thus, our study demonstrated that the m⁶A modification is crucial for the control of trophoblast invasion and that this regulation is disrupted in RM diseases. RM patients had significantly higher expression of the m⁶A demethylase ALKBH5 in chorionic villous tissue than normal controls; this result is consistent with the finding that ALKBH5 overexpression inhibits trophoblast invasion and decreases RNA m⁶A methylation levels. Furthermore, using RNA-sequencing experiments, we identified the impact of ALKBH5 on the expression of CYR61 in trophoblast. These results suggested that ALKBH5 plays a key role in the pathogenesis of RM by regulating trophoblast invasion.

Methods and materials

Patient Characteristics

Between July 2016 and April 2018, 69 patients with RM (23-38 years old; mean age, 30.6 ± 7.4 years) who had been treated at the Department of Obstetrics and Gynaecology at Shanghai First Maternity and Infant Hospital at the Tongji University School of Medicine, were included in this study. Patients with the following features were excluded: (1) presence of uterine abnormalities or cervical incompetence on pelvic examination and ultrasound, (2) abnormal karyotype analysis of the parents or abortus, (3) comprehensive hormonal status assessment to rule out luteal phase defects, hyperprolactinaemia and hyperandrogenaemia, and (4) symptoms of endocrine or metabolic diseases (e.g., diabetes, hyperthyroidism, and hypothyroidism).

Additionally, 65 women aged 22-38 years (mean age, 30.3 ± 7.9 years) with normal early pregnancies

were recruited as healthy controls. All women have had previous pregnancies without any history of spontaneous abortion, preterm labor, or preeclampsia. All women recruited to the control group had undergone artificial abortions to terminate their unwanted pregnancies at 6-10 weeks of gestation, and villous tissue samples were collected from these patients, and the samples treated for isolation of primary trophoblast or stored in liquid nitrogen until analysis. The study protocol was approved by the Medical Ethics Committee of the Shanghai First Maternity and Infant Hospital, Shanghai. Written informed consents were obtained from all the participants before enrolment.

Cell Culture

Primary trophoblast were isolated by trypsin-DNase I digestion (Sigma-Aldrich, St. Louis, MO) and discontinuous Percoll (GE Healthcare, Amersham Place, UK) gradient centrifugation from pooled villi obtained from 3-5 patients, as previously described [26]. The resultant trophoblast cell culture had a purity of approximately 95%, which was determined by flow cytometry for cytokeratin-7 positive, HLA-G positive, and vimentin negative cells. Purified trophoblast were seeded in the wells of 12-well plates at a concentration of 4×10^5 cells/mL and cultured in Dulbecco's modified Eagle's Medium (DMEM)/F12 (GE Healthcare) plus 10% fetal bovine serum (FBS; Gibco, Carlsbad, CA, USA) for further experiments.

The HTR-8/SVneo cell line [27], which is derived from human invasive EVT, was a kind gift from Dr. PK Lala (University of Western Ontario, London, Ontario, Canada). The cells were cultured in DMEM/F12 with 10% fetal bovine serum (FBS) plus Penicillin/ Streptomycin antibiotics (Invitrogen, Carlsbad, CA, USA). JEG-3 cells, a human choriocarcinoma cell line, were obtained from the cell bank at the Chinese Academy of Sciences (Shanghai, China) with the original source being the American Type Culture Collection (ATCC) (Manassas, VA, USA) and cultured in 1640 complete medium supplemented with 10% FBS plus Penicillin/ Streptomycin antibiotics in 5% CO₂ at 37 °C.

Overexpression of ALKBH5

The pLV-EGFP-T2A-Puro-hALKBH5 plasmid and the control vector were purchased from Cyagen company, and GV141-CYR61 plasmid and the control vector were purchased from Shanghai Genechem company, the plasmids were purified using an Endofree Plasmid kit (Qiagen, Hilden, Germany) and transfected into the cells using a jetPRIME® kit (Polyplus, Illkirch, France). For lentivirus construction, the pLV-EGFP-T2A-Puro-hALKBH5

plasmid co-transfected with VSVG and Δ8.9 plasmids into HEK293 cells for 48 h to produce lentivirus overexpressing ALKBH5.

Knockdown of ALKBH5 and CYR61

ALKBH5 or *CYR61* knockdown was performed using specific small interfering RNA specific for *ALKBH5* (siALKBH5 or siCYR61). Unless otherwise indicated, all oligonucleotides were purchased from GenePharma Inc., and transfected into the cells at a final concentration of 100 nM/L using Oligofectamine reagent (Invitrogen, Carlsbad, CA, USA).

Explant Culture

Small 2-3 mm tissue sections were obtained from the tips of first-trimester human placental villi (6-10 weeks), dissected, and explanted in 24-well culture dishes pre-coated with phenol red-free Matrigel® substrate (Corning Life Sciences, New York, NY), as previously described [28]. Coated inserts were placed into 24-well culture dishes (Costar, Cambridge, MA). Villi explants were cultured in DMEM/F12 media containing 10% FBS. Placental villi that successfully anchored on Matrigel matrix and initiated outgrowth were used for the subsequent experiments, and are referred to as 24 h samples. EVT sprouting and migration from the distal end of the villous tips were recorded daily for up to 3 days. The extent of migration was measured via using ImageJ Pro 6.0 software. To test the effect of ALKBH5 on the migration of EVTs, 250 nM siRNA specifically targeting ALKBH5 or an equal concentration of control siRNA was introduced into two wells of extravillous explants from HCs or RM patients. The images were obtained after 24 h and 72 h of *in vitro* culture under a light microscope. Extravillous explants from HCs were incubated with lenti-ctrl or lenti-ALKBH5 lentiviral, and images after 24 h and 72 h of *in vitro* culture were taken under a light microscope. All explant experiments with cultured villi were repeated three times.

ALKBH5 knockdown Transcriptome sequencing

A total amount of 3 µg RNA per sample was used as input material for the RNA sample preparations. Sequencing libraries were generated using NEBNext® Ultra™ RNA Library Prep Kit for Illumina® (NEB, USA) following manufacturer's recommendations and index codes were added to attribute sequences to each sample. The PFKM was assessed and log₂ transformed, the data was further calculated and displayed as heatmaps to help visualize differential expression. Details are provided in the Supplementary materials and methods.

Quantitative Real-time PCR

Total RNA was extracted from cultured cells or primary cells using the TRIzol reagent (Life Technologies, Grand Island, NY), according to the manufacturer's instructions, and used to generate cDNA with a 5 × All-In-One RT MasterMix from Applied Biological Materials Inc (Richmond, BC, Canada). Realtime-PCR (qRT-PCR) was performed using SYBR Green kit (Qiagen, Hilden, Germany). For in vitro experiments, relative expression was calculated using the $2^{-\Delta\Delta C_t}$ method and normalized to the internal control gene *GAPDH* mRNA (human). For clinical data, relative expression was calculated using the $2^{-\Delta C_t}$ method and normalized against *GAPDH* mRNA values. The primers used are shown in Supplementary Primers.

MeRIP-qPCR.

For quantification of m⁶A-modified CYR61 levels, methylated RNA immunoprecipitation was performed. Total RNA was isolated from HTR-8 cells by Trizol. 3 μg of anti-m⁶A antibody (Millipore, ABE572) or anti-IgG (Cell Signaling Technology) was conjugated to protein A/G magnetic beads in IP buffer (20 mM Tris pH 7.5, 140 mM NaCl, 1% NP-40, 2 mM EDTA) for overnight at 4 °C. A 100 μg aliquot of total RNA was then incubated with the antibody in IP buffer supplemented with RNase inhibitor and protease inhibitor. RNA was eluted from the beads by incubating with 200 μl 0.5 mg/mL N⁶-methyladenosine 5-monophosphate sodium salt (Sigma-Aldrich) for 1 h at 4 °C. Total RNA was eluted with elution buffer, purified through phenol-chloroform extraction. For further qRT-PCR assay, 10 ng of eluate or input total RNA was reverse-transcribed using Superscript III with random hexamers, and enrichment of m⁶A-containing transcripts. Fold enrichment was calculated by calculating the $2^{-\Delta C_t}$ of eluate relative to the input sample. The primers used for PCR were as follows: CYR61 primer for MeRIP-qPCR #1 F: 5'-GAATGCAGCAAGACCAAGAAAT-3', R: 5'-ACGCAGTACTTGGGCCGGTAT-3'; CYR61 primer for MeRIP-qPCR #2 F: 5'-TTTCCAAGAACGTCATGATGAT-3', R: 5'-CCTGGAAACC-CAGGTAGCAT-3'.

Statistical Analysis

All statistical values were calculated using SPSS 22.0 (Chicago, IL, USA). Experimental studies were analyzed by independent sample *t*-test for the comparison between 2 groups, and by one-way ANOVA followed by post-hoc Tukey's test for the comparison among multiple groups. For clinical studies, the nonparametric Mann-Whitney test was used to compare ALKBH5 and CYR61 expression.

Correlations were analyzed using the Spearman's rank correlation test. Data are presented as mean ± SD. All *P* values are two-sided. A *P* value of < 0.05 was considered statistically significant.

Results

RM is associated with high levels of m⁶A mRNA methylation

A previous study demonstrated that insufficient proliferation and invasion of cytotrophoblasts (CTBs) is associated with early or late RM [29]. To explore whether mRNA m⁶A methylation is involved in the pathogenesis of RM, we analyzed the expression profiles of m⁶A 'writer', 'eraser', and 'reader' associated genes in chorionic villous tissues derived from RM patients (*n* = 12) and HCs (*n* = 12) using qRT-PCR. Our results showed that *ALKBH5* mRNA expression was significantly increased in the chorionic villi of RM patients compared to HCs (Figure 1A). In contrast, level of *YY1* and *CGB* mRNA expression, which was reported in our previous paper [26], was significantly decreased in the chorionic villi of RM patients compared to HCs. We further examined the expression levels of m⁶A and *ALKBH5* mRNA in chorionic villi from RM patients (*n* = 65) and HCs (*n* = 57). Consistently, we found a significantly higher *ALKBH5* mRNA level and a significantly lower m⁶A level in the chorionic villi from the RM group compared to the HC group (Figures 1B-C). Linear correlation analysis showed that the *ALKBH5* mRNA level was negatively correlated with the mRNA m⁶A level in villous tissue (Figure 1D). These results suggest that *ALKBH5* inhibits RNA m⁶A methylation in trophoblasts from RM patients. Furthermore, immunohistochemical analysis of paraffin-embedded first-trimester chorionic villous tissues was performed to investigate the localization of *ALKBH5* in chorionic villous tissue. *ALKBH5* expression in normal chorionic villous tissue from HCs was primarily observed in the nucleus of cytotrophoblasts (CTBs). A stronger positive signal for *ALKBH5* was detected in chorionic villous tissue from the RM group compared to the HC group (Figures 1E-F). These findings were confirmed by western blotting and qRT-PCR analysis, which showed that *ALKBH5* was expressed at a higher level in primary trophoblast of RM patients than HCs (Figure 1G-H). Collectively, these results indicate that *ALKBH5* expression is increased in trophoblast in RM patients and suggest that this increase may be correlated with trophoblast function.

ALKBH5 regulates trophoblast invasion at the maternal-fetal face

To directly address the role of *ALKBH5* in human trophoblast, the HTR-8/SVneo (HTR-8) cell

line, a first-trimester human extravillous trophoblast-derived cell line, was transfected with siALKBH5 oligonucleotides or with the ALKBH5-expressing vector. ALKBH5 expression was reduced after siALKBH5 transfection and was increased after transfection with the ALKBH5 expression vector

(Figures 2A-C). Further, Matrigel® invasion assays revealed that overexpression of ALKBH5 significantly inhibited the invasive ability of HTR-8 cells, whereas knockdown of ALKBH5 significantly promoted cell invasion (Figures 2D-G).

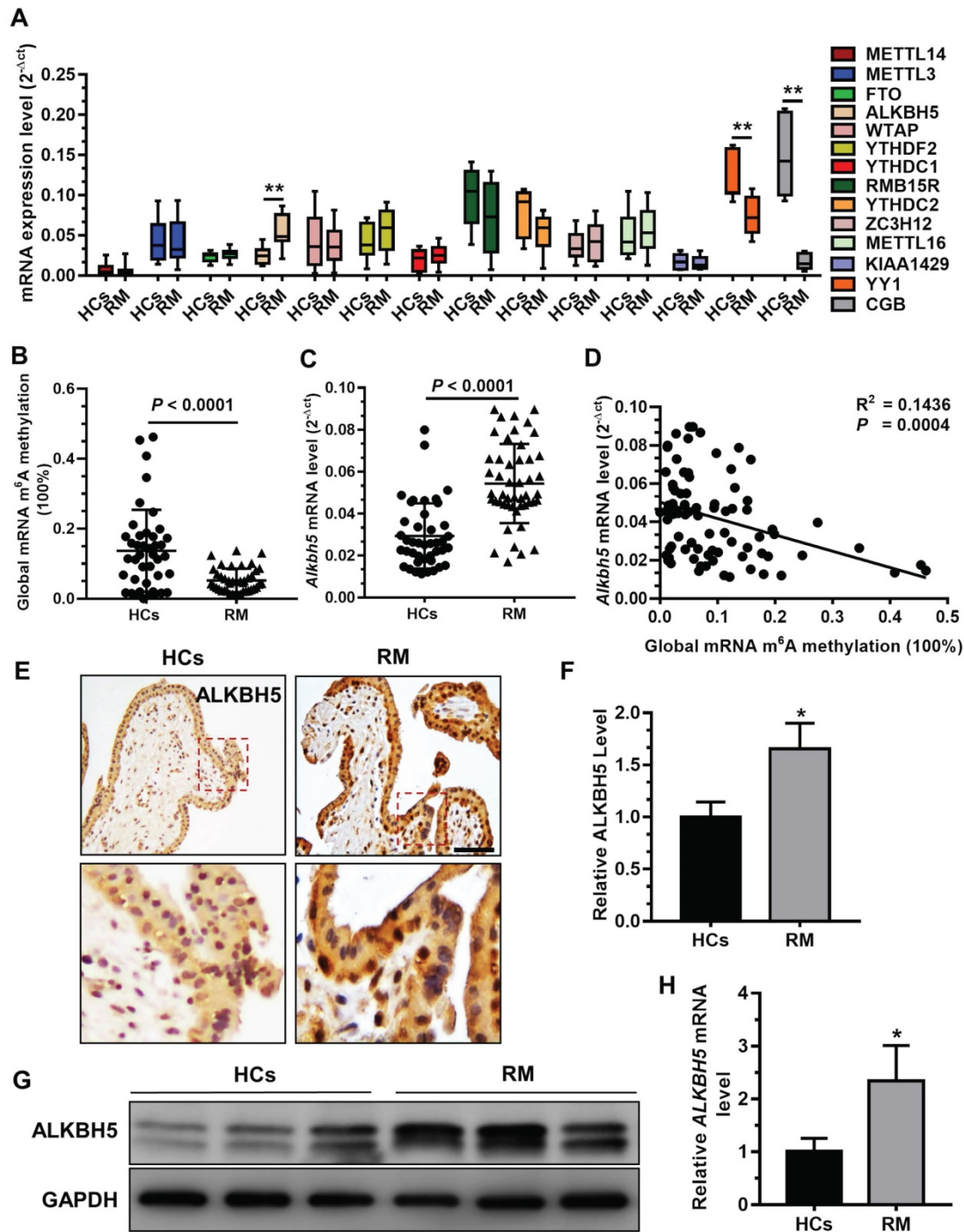


Figure 1: ALKBH5 is overexpressed in first-trimester placental trophoblast from recurrent miscarriages patients. (A) Expression of RNA m⁶A methylation-regulated associated genes was determined in first-trimester human villous tissues from patients with RM or in healthy controls (HCs) using quantitative RT-PCR (qRT-PCR). (B) Global RNA m⁶A methylation of villous tissues from patients with RM or in HCs was assessed using the EpiQuik m⁶A RNA methylation quantification ELISA kit. (C) The ALKBH5 mRNA expression levels in the villous tissues of patients with RM (n = 65) and HCs (n = 57) were determined by qRT-PCR. (D) Global RNA m⁶A methylation level was measured in the villous tissues of patients with RM and HCs by EpiQuik m⁶A RNA methylation quantification ELISA kit and was correlated to level of ALKBH5 mRNA expression. (E and F) Single staining of maternal villi (cytotrophoblasts and syncytiotrophoblasts) using anti-IgG (rabbit) or anti-ALKBH5 antibody (rabbit), which was visualized with a labeled streptavidin biotin horseradish peroxidase (HRP) kit. Sections were counterstained with hematoxylin, and positive cells were quantified using Image-Pro Plus 6.0 software (n = 19); Right scale bar = 100 μ m. (G and H) Primary trophoblasts were isolated from first-trimester villi of RM patients and HCs, and ALKBH5 levels were determined by western blotting and qRT-PCR.

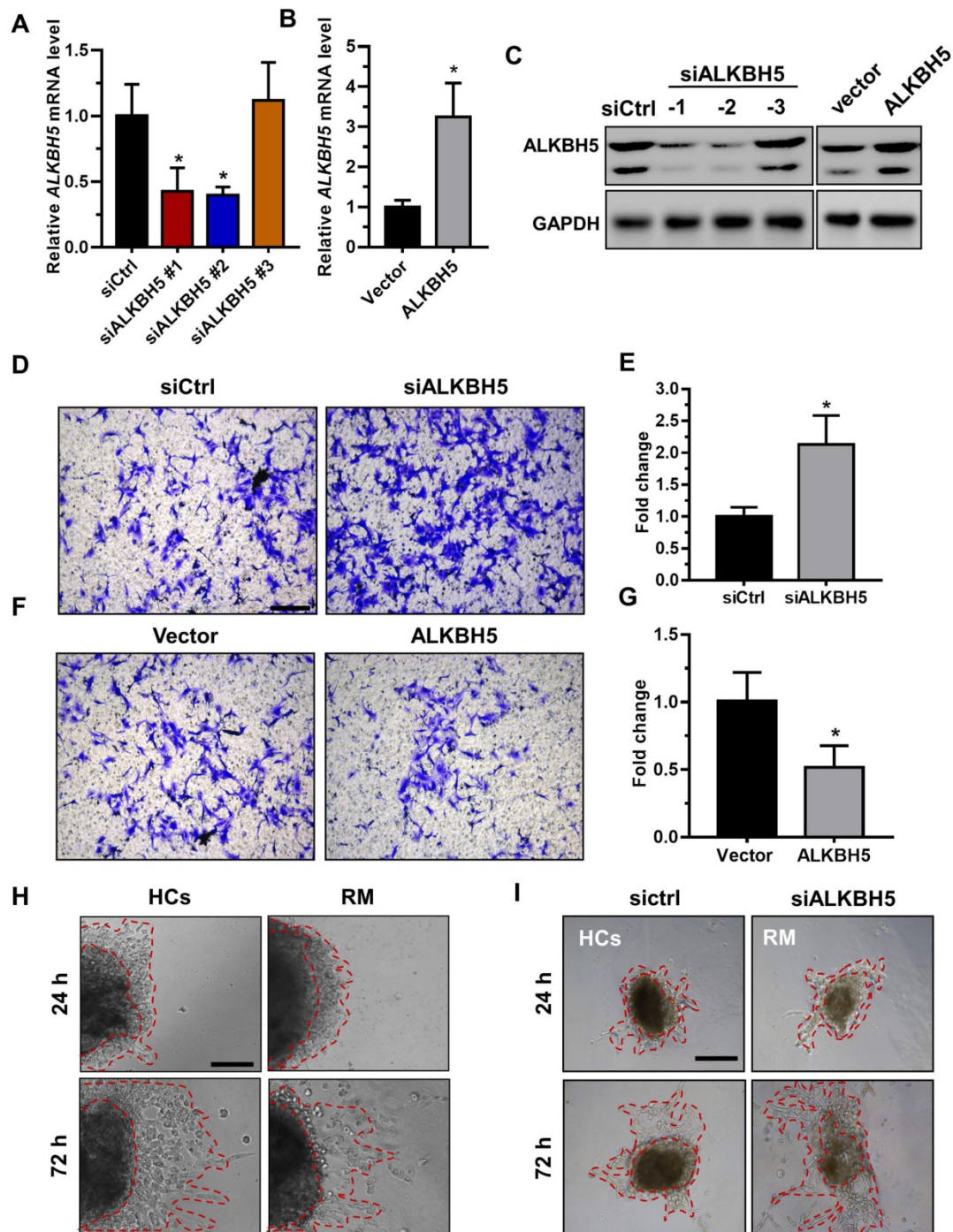


Figure 2: ALKBH5 inhibits trophoblast invasive ability *in vitro* and trophoblast outgrowth in a villous explant culture model. (A and B) QRT-PCR and western blotting analyses were performed to determine the levels of ALKBH5 in HTR-8 cells transfected with siCtrl, siALKBH5-1, siALKBH5-2, siALKBH5-3, control vector, or ALKBH5-overexpressing vector after 48 h. (D and E) ALKBH5 knockdown in HTR-8 cells increased trophoblast invasion compared to that of the control cell line. The invasive ability of the cells was assessed by Image-Pro Plus 6.0 software. (Panel: original magnification \times 200 magnification). (F and G) ALKBH5 overexpression significantly reduced cell invasion compared to that of the vector control cell line. The invasive ability of the cells was assessed by Image-Pro Plus 6.0 software. (Panel: original magnification \times 200 magnification). (H) Extravillous explants were obtained from HCs and RM patients at 6-10 weeks of gestation and cultured on Matrigel. Serial pictures of the explants were taken under a light microscope after 24 h and 72 h of culture *in vitro*. (I) Extravillous explants from RM at 6-10 weeks of gestation were maintained in culture on Matrigel. Serial pictures of the explants transfected with siALKBH5 or siCtrl were taken under a light microscope after 24 h and 72 h of culture *in vitro*.

Extravillous explants from first-trimester villi from the RM and age- and gestational week-matched control groups were cultured on Matrigel-coated dishes. The distance of outgrowth on the Matrigel surface was measured at 24 h and 72 h. Following 24 h of culture, the explants were anchored into the

Matrigel and started to exhibit outgrowth. No significant difference was observed between the control and RM groups at this point. At 72 h of *in vitro* culture, the RM explants had migrated shorter distances than the control explants (Figure 2H and Figure S1A). To further confirm the role of ALKBH5

in trophoblast invasion, we cultured explants freshly obtained from the RM villous tissue samples (6-10 weeks of gestation) in 24-well dishes for 24 h and then treated them with siCtrl and siALKBH5 oligonucleotides. The results showed that the explants treated with siALKBH5 migrated significantly farther than the siCtrl-treated explants (Figure 2I and Figure S1B). Therefore, these results clearly suggest that ALKBH5 plays an important role in the regulation of trophoblast invasion.

The m⁶A modification is enriched in CYR61

To further elucidate the molecular mechanism underlying ALKBH5 regulation of trophoblast invasion, we transfected HTR-8 cells with siALKBH5 oligos for 48 h. Transcriptome RNA sequencing was employed to identify genes dysregulated by ALKBH5 knockdown in HTR-8 cells. A total of 6891 genes were found to be dysregulated after ALKBH5 knockdown. Of these, 3383 were upregulated and 3408 were downregulated (Figure 3A), the majority of which had a fold change value (siALKBH5/siCtrl) between 0.5 and 2 after ALKBH5 knockdown. Supplemental Table S1 provides detailed gene quantitation information from the three replicate experiments. We next selected 33 genes based on transcriptome analysis for validation. Although there were differences in the fold changes of some genes between the RNA sequencing data and the qRT-qPCR validation data, 20 phenotypically relevant genes all exhibited changes in the same direction (Figures 3B-C), suggesting a significant impact of ALKBH5 on these mRNAs expression. Furthermore, HTR-8 cells were transfected with ALKBH5-expressing plasmid for 48 h, and qRT-PCR clearly showed that the *MET*, *FGF1*, *WDFY1*, and *HEG1* transcripts were increased in trophoblasts from the ALKBH5 overexpression group. In contrast, *FN1*, *CYR61*, *CTGF*, and *TPM4* transcripts were obviously decreased in trophoblast from the ALKBH5 overexpression group (Figure 3D). Furthermore, we determined the m⁶A modification of *MET*, *FGF1*, *WDFY1*, *HEG1*, *FN1*, *CYR61*, *CTGF*, and *TPM4* by performing methylated RNA immunoprecipitation (MeRIP) experiments. Interestingly, *CYR61* was significantly enriched in the anti-m⁶A group compared with the IgG group (Figure 3E). To define the potential functions of m⁶A-modified *CYR61*, using SRAMP online tool (A sequence-based N⁶-methyladenosine (m⁶A) modification site predictor) [30], we analyzed the m⁶A sites located in *CYR61* and found five RRACH m⁶A sequence motifs in the 3'-untranslated regions (3'-UTR) proximal to the stop codon, which was previously described as a location for m⁶A deposition (Figure S2). To further characterize the m⁶A

methylation of *CYR61*, we performed siRNA-mediated downregulation of ALKBH5, an important component of the m⁶A demethylase complex, in trophoblast. The MeRIP results showed that ALKBH5 knockdown significantly increased the enrichment of *CYR61* mRNA in the anti-m⁶A group compared with the IgG group (Figure 3F). ALKBH5 overexpression decreased the enrichment of *CYR61* mRNA (Figure 3G). We further detected the m⁶A methylation of *CYR61* mRNA in villous from HCs and RM patients, the MeRIP-PCR result showed that enrichment of *CYR61* mRNA was higher in HCs group compared with RM patients group (Figure 3H). These data indicate that ALKBH5 regulates the expression of *CYR61* mRNA in an m⁶A-dependent manner.

M⁶A methylation specifically controls CYR61 expression and stability in trophoblasts

To determine the underlying mechanisms of decreased *CYR61* expression upon increased m⁶A methylation, we measured the m⁶A levels in primary trophoblast transfected with ALKBH5-expressing plasmid or ALKBH5 siRNA. The results showed that ALKBH5 overexpression resulted in a significant reduction in the RNA m⁶A methylation of primary trophoblast, as indicated by m⁶A RNA methylation quantification (colorimetric) analysis (Figure 4A), whereas ALKBH5 knockdown increased the RNA m⁶A methylation level (Figure 4B). QRT-PCR results showed that ALKBH5 knockdown significantly promoted *CYR61* mRNA expression in HTR-8 cells, while ALKBH5 overexpression decreased its expression (Figures 4C-D). Further, western blotting results showed that ALKBH5 knockdown significantly promoted expression of *CYR61* protein in HTR-8 cells and JEG-3 cells, while overexpression of ALKBH5 decreased its expression (Figures 4E and Figure S3). We further explored the mechanism by which m⁶A methylation regulates mRNA stability. The mRNA half-life of *CYR61*, *FGF1*, *CTGF* and *MET* was assessed in the ALKBH5 siRNA-transfected trophoblast using an actinomycin D chase experiment and a one-phase exponential decay model with *GAPDH* mRNA normalization. This experiment revealed the strong impact of ALKBH5 on *CYR61* mRNA stability, but did not affect *FGF1*, *CTGF* and *MET* mRNA stability. The half-life of *CYR61* mRNA was approximately 4.3 h after siRNA control transfection; the half-life was increased when cells were transfected with siALKBH5 oligos (5.4 h) (Figure 4F and Figure S4). The half-life of *CYR61* mRNA was further assessed in the ALKBH5-expressing trophoblast. The half-life of *CYR61* was 4.5 h after vector control transfection, and the half-life was

decreased by almost 1.5 times when cells were transfected with the ALKBH5 vector (3.2 h) (Figure 4G). To further elucidate the molecular mechanism of m⁶A regulation of CYR61 mRNA stability, we performed the CYR61 3' UTR-reporter luciferase assay and found that ALKBH5 knockdown increased the activity of the luciferase construct containing the

CYR61 3'UTR. Mutation at all of these sites (A to T) almost completely rendered resistance to the luciferase activity of ALKBH5 knockdown (Figures 4H-I). These results suggest that ALKBH5 regulates CYR61 post-transcriptionally via an m⁶A methylation-dependent mechanism.

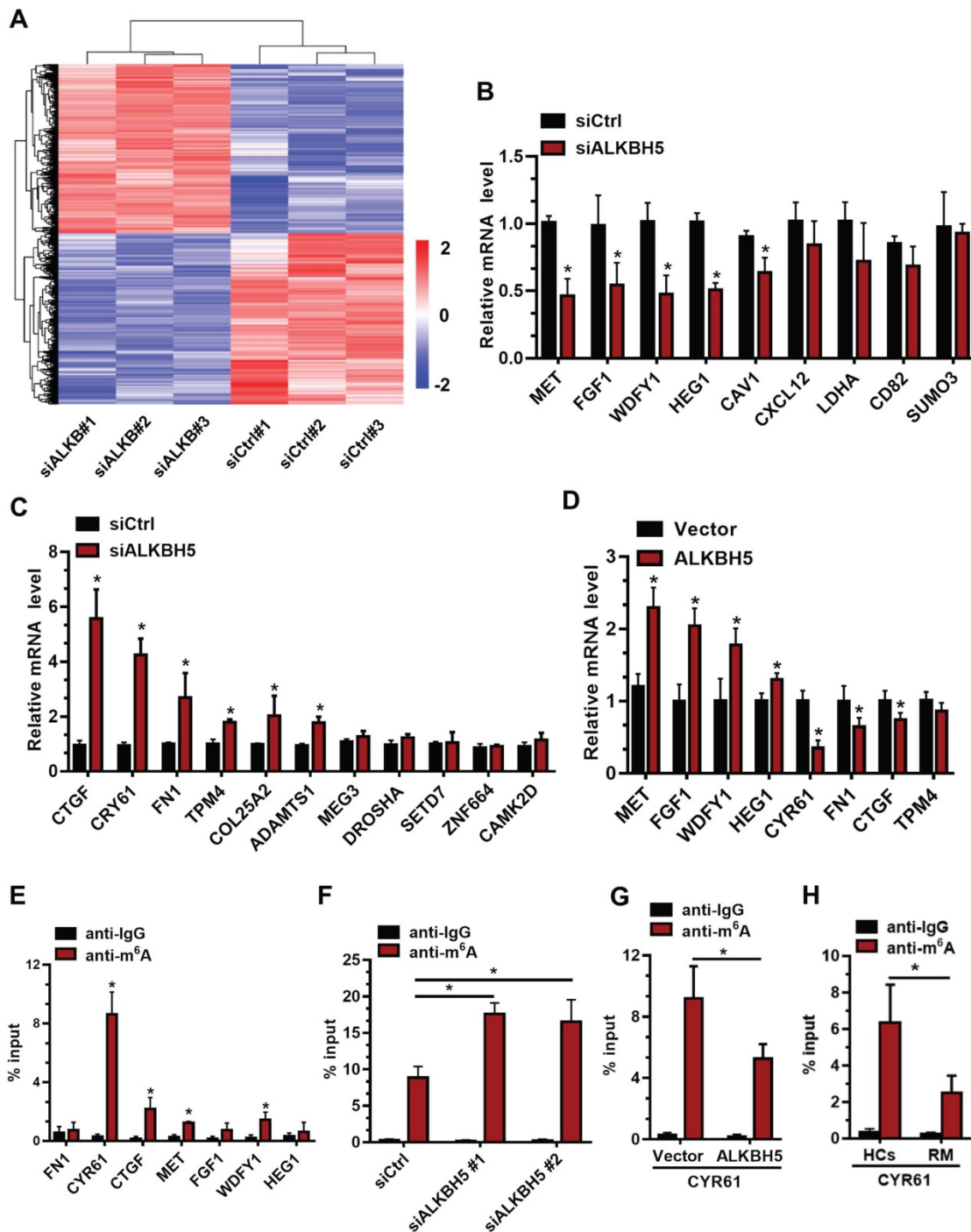


Figure 3: CYR61 is a downstream target of m⁶A in trophoblast. (A) Heatmap of normalized gene expression levels of HTR-8 cells transfected with siCtrl or siALKBH5. Blue indicates down-regulation of genes expression; Red indicates up-regulation of genes expression. (B and C) QRT-PCR was performed to determine the mRNA levels of the selected genes in HTR-8 cells transfected with siCtrl or siALKBH5. (D) QRT-PCR was performed to determine the mRNA levels of selected genes in HTR-8 cells transfected with vector or ALKBH5-expressing plasmid. (E) Enrichment of m⁶A-modified CYR61, CTGF, MET and WDFY1 in HTR-8 cells. The percentage of the input is shown. *P < 0.05 versus anti-IgG. (F) Changes in m⁶A-modified CYR61 level upon ALKBH5 knockdown. The percentage of the input is shown. *P < 0.05 versus siCtrl. (G) Changes in m⁶A-modified CYR61 level upon ALKBH5 overexpression. The percentage of the input is shown. *P < 0.05 versus vector. (H) Changes in m⁶A-modified CYR61 level upon HCs and RM. The percentage of the input is shown. *P < 0.05 versus HCs.

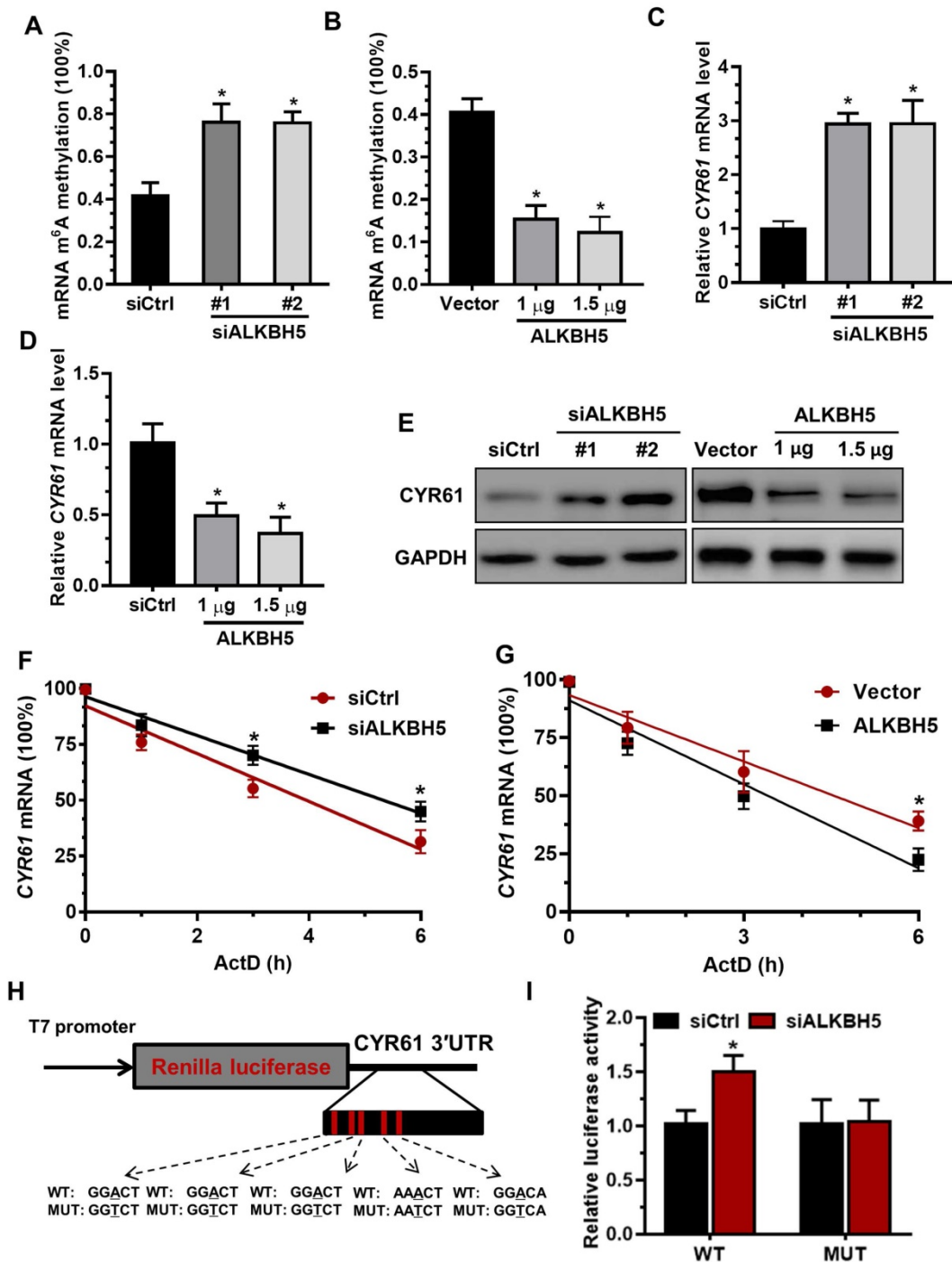


Figure 4: The m⁶A mark is critical for CYR61 expression and stability in trophoblasts. (A and B) RNA m⁶A RNA methylation of primary trophoblast transfected with siALKBH5 or ALKBH5-expressing plasmid was assessed using the m⁶A RNA Methylation Quantification ELISA kit. (C-E) Western blotting and qRT-PCR analysis of CYR61 expression in HTR-8 cells transfected with siCtrl, siALKBH5 #1, siALKBH5 #2, control vector, or ALKBH5-expressing plasmid after 48 h. (F and G) HTR-8 cells were transfected with siCtrl, siALKBH5, vector or ALKBH5-expressing plasmid for 36 h; a time course for mRNA stability was initiated by adding an RNA-Polymerase II inhibitor [actinomycin D (5 μg/mL)]. Cells were harvested at the indicated time points. Expression levels were normalized to that at “0 hour”, and GAPDH mRNA was used as the reference gene. The results are shown as the mean of at least three independent experiments. *P < 0.05 versus the vector or siCtrl. (H and I) A schema for the constructs and co-transfection experiments, a fragment of 3'-UTR of CYR61 (wild-type and mutant) was cloned into a psiCheck2 vector, downstream of the renilla luciferase gene. These construct were co-transfected with the siALKBH5 or siCtrl into HTR-8 cells. Cells were harvested after 24 h. Renilla luciferase activity was measured and normalized to that of firefly luciferase. The results are represented as the mean of three independent experiments. *P < 0.05 versus the siCtrl.

CYR61 is a functional target of ALKBH5 in trophoblast

To further assess the relationship between ALKBH5 and the regulatory functions of CYR61 in trophoblast, we cultured explants freshly obtained

from the HC villous tissue samples in 24-well dishes for 24 h, and then treated them with siCtrl, siALKBH5, lenti-ctrl or lenti-ALKBH5 lentivirus. Explants treated with lenti-ALKBH5 migrated significantly slower than the lenti-ctrl-treated explants

group. By contrast, explants treated with siALKBH5 migrated significantly farther than the siCtrl-treated explants group (Figures 5A-B and Figure S5). Furthermore, whole-mount immunofluorescence staining of villous samples from both groups was performed to detect CYR61 expression and CK-7 was

used as a marker of EVT invasion and migration. The CYR61 levels were significantly decreased in the EVT of villous tissues from the lenti-ALKBH5-treated group compared with the lenti-ctrl-treated group (Figure 5C).

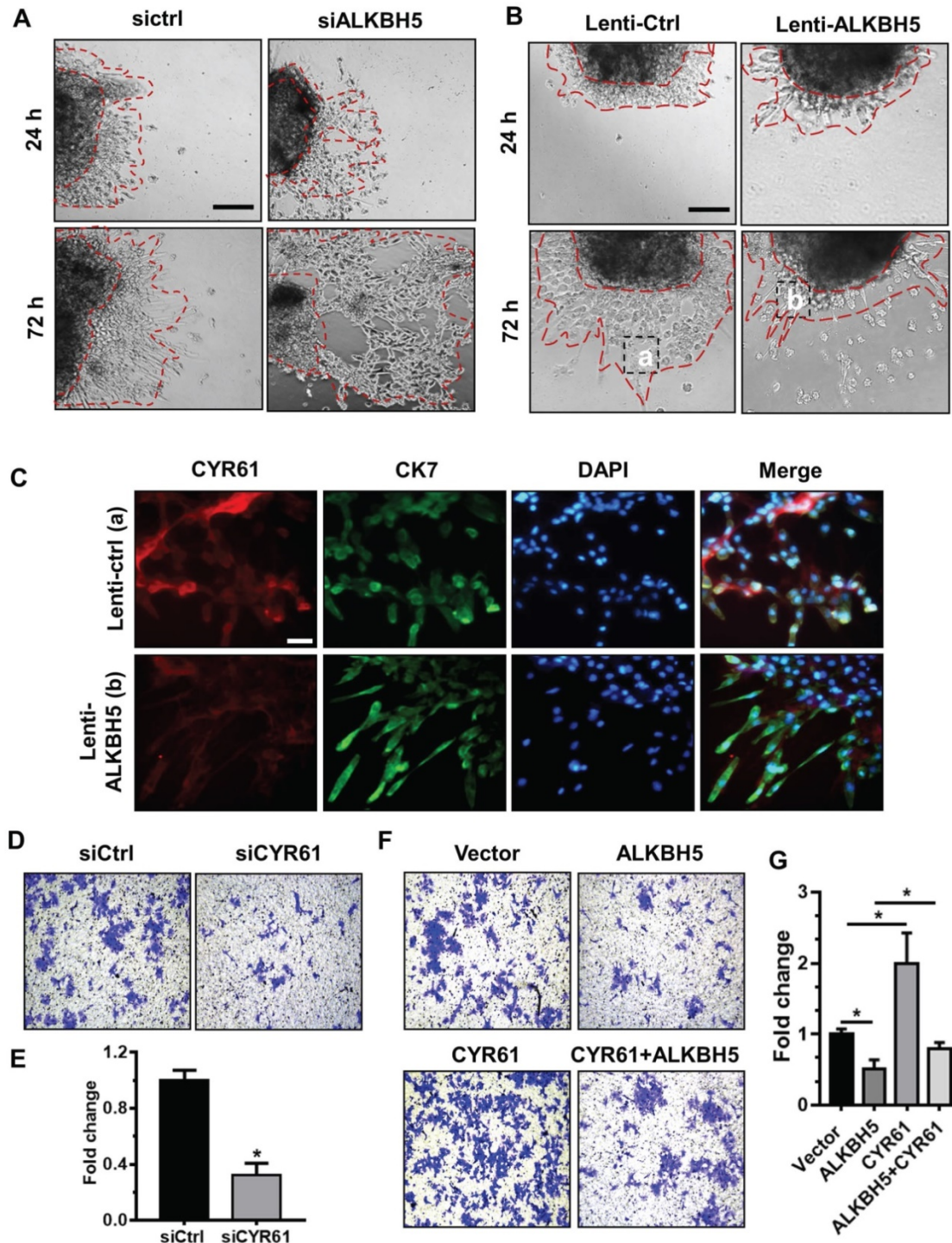


Figure 5: ALKBH5 promotes trophoblast invasion by upregulating CYR61 expression. (A and B) Extravillous explants from HCs were maintained in culture on Matrigel. Serial pictures of the explants incubated with siCtrl, siALKBH5, lenti-ctrl or lenti-ALKBH5 lentivirus were taken under a light microscope after 24 h and 72 h of culture *in vitro*. (C) Immunofluorescence staining using anti-CYR61 antibodies showed an obvious decrease in the CYR61 level in the ALKBH5 overexpression group (b) compared with the vector group (a). Green fluorescence signals indicate bound anti-CK-7 antibodies; CYR61 staining is visualized as red; and the DAPI-stained nuclei are blue. (D and E) HTR-8 cells were transfected with siCtrl or siCYR61 for 24 h. The invasive ability of the cells was assessed by Image-Pro Plus 6.0 software. * $P < 0.05$ compared with the siCtrl. (F and G) HTR-8 cells were transfected with vector or ALKBH5 and CYR61 expression vectors or with the ALKBH5 + CYR61 expression vector for 24 h. The invasive ability of the cells was assessed by Image-Pro Plus 6.0 software. * $P < 0.05$ versus the vector.

To further confirm the role of CYR61 in trophoblast invasion, western blotting analysis was used to analyze the level of CYR61 in HTR-8 cells transfected with siCYR61 or *CYR61* overexpression vectors. *CYR61* knockdown or *ALKBH5* overexpression decreased expression of CYR61, while *CYR61* overexpression significantly enhanced expression of CYR61. Overexpression of CYR61 could rescue the level of CYR61 protein decreased by *ALKBH5* overexpression (Figure S6). Furthermore, the Matrigel cell invasion assays results revealed that CYR61 knockdown significantly decreased the invasive ability of trophoblast (Figures 5D-E). Additionally, *CYR61* overexpression effectively reversed the reduction in trophoblast invasion caused by *ALKBH5* overexpression (Figures 5F-G). These results indicate that *ALKBH5* regulates trophoblast invasion via downregulation of *CYR61* expression.

CYR61 expression correlates negatively with ALKBH5 expression in RM patients

To further clarify the clinical significance of CYR61 in RM patients, we evaluated CYR61 expression using qRT-PCR and western blot analyses of first-trimester chorionic villi tissues to determine whether CYR61 is involved in the pathogenesis of RM. *CYR61* expression was significantly downregulated in villous tissue of RM patients (Figures 6A-B). Double immunofluorescence staining for *ALKBH5* and CYR61 revealed increased staining for *ALKBH5* and decreased staining for CYR61 in CTBs from villous tissues of the RM group compared with that of the HC group (Figure 6C). Linear correlation analysis showed that the *CYR61* mRNA level was positively correlated with global RNA m⁶A methylation in villous tissue (Figure 6D), while the *CYR61* mRNA level was negatively correlated with the *ALKBH5* mRNA level in villous tissue. These results suggest that *ALKBH5* and CYR61 expression levels are negatively associated in the villous tissue of the RM group, which correlated with the pathogenesis of RM.

Discussion

RM affects approximately 1-3% of women during their reproductive years and is usually defined as three or more consecutive spontaneous abortions before 20 weeks of gestation [31]. RM is associated with substantial adverse clinical and psychological consequences for women and their families. Various therapeutic strategies to increase the rate of live births among these women have been evaluated, but no effective treatment has been identified [32]. Moreover, RM is also associated with a high level of psychological distress. Thus, comprehensive

molecular studies are needed to elucidate the causes of RM and to develop potential targets. However, the underlying molecular mechanism of RM remains poorly understood. Currently, many studies have found that insufficient proliferation and invasion of trophoblasts are associated with early and late RM [29, 33]. In this study, we explored the function of *ALKBH5* in human villi and trophoblast during the early stage of pregnancy.

ALKBH5 RNA demethylase belongs to the AlkB subfamily of the Fe (II)/2-oxoglutarate (2OG) dioxygenase superfamily and is primarily localized in the nucleus. This enzyme is upregulated under hypoxic conditions by the hypoxia-inducible factor (HIF) transcription factor pathway [17]. *ALKBH5* was observed to be highly expressed in the lung, followed by the testis, pancreas, spleen and ovary, but has low expression in the heart and brain [16, 34]. Interestingly, *ALKBH5* may function differently in distinct types of diseases. *ALKBH5* functions as an oncoprotein in GBM and breast cancer [17, 18]; it may exert a tumor-suppressor role in AML as implied by its frequent copy number loss and low expression level in AML [35]. In this study, we first found that the *ALKBH5* level was higher in the placental tissue from RM patients than that of age- and gestational-matched HCs, suggesting that *ALKBH5* is disrupted under pathological conditions. Moreover, multiple lines of evidence, including *in vitro* cell migration and invasion assays, *in vivo* extravillous explant culture experiments, and analyses of human RM specimens, support the role of *ALKBH5* in mediating trophoblast via regulating CYR61 expression. Therefore, these data demonstrate that *ALKBH5* could play an important role in trophoblast invasion. This is in contrast to previous result, which reports *ALKBH5* functions as an oncogene in GBM and breast cancer. It is possible that *ALKBH5* could play different functions in the different cell context, likely through regulating distinct sets of targets. Thus, more detailed studies are warranted to explore the biological function of each individual m⁶A regulatory genes in different types of cell, and to identify their core target genes to elucidate the underlying molecule mechanisms.

During placental development, continuous invasion of trophoblasts into the maternal compartment depends on the support of proliferating EVT. Impairment of EVT invasion predisposes a pregnancy to uteroplacental insufficiency and results in a significantly increased risk of preeclampsia, fetal growth restriction (FGR), and early RM [36-38]. Recently, CYR61 was shown to facilitate the migration and invasion of trophoblastic cells. CYR61 enhanced the migratory capability of trophoblast cells via the

activation of FAK and Akt kinase [24]. Here, we found that elevated ALKBH5 impaired trophoblast invasion by inhibiting the RNA m⁶A methylation level, which reduced the expression of CYR61. We further used gain- and loss-of-function analyses, MeRIP, and RNA decay analyses to demonstrate that ALKBH5 regulates CYR61 stability and expression in trophoblast via an m⁶A methylation-dependent mechanism. Together, these findings indicate that ALKBH5 might be involved in the progression of RM by modulating CYR61 expression.

In summary, this study provides new insight into the pathogenesis of RM by elucidating the role of ALKBH5, which was found to regulate trophoblast invasion in early pregnancy through its effects on

mRNA m⁶A methylation. We also showed that ALKBH5 controlled CYR61 mRNA stability by regulating m⁶A methylation and that the downstream effects of ALKBH5 and CYR61 might be related. Thus, ALKBH5 and CYR61 may be involved in the pathogenesis of RM, and therefore, therapeutic methods that target these two factors may be effective for the treatment of RM.

Abbreviations

RM: recurrent miscarriage; HCs: healthy controls; m⁶A: N6-methyladenosine; ALKBH5: alkylation repair homolog 5; CYR61: cysteine-rich 61; MeRIP: methylated RNA immunoprecipitation.

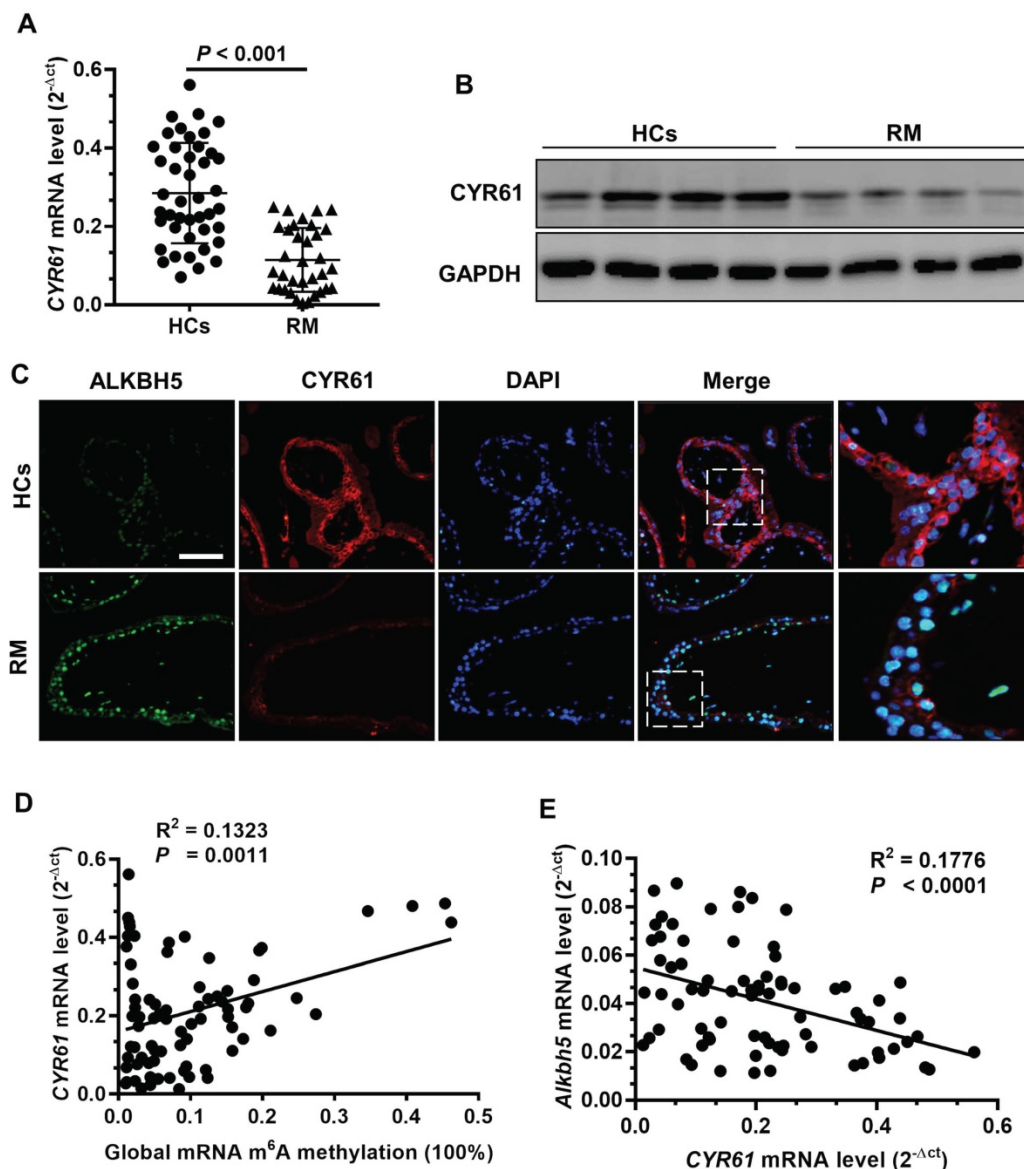


Figure 6: ALKBH5 expression is negatively correlated with CYR61 expression in RM disease. (A) CYR61 mRNA levels in first-trimester human villous tissues from RM patients ($n = 65$) or in HCs ($n = 57$) were determined by qRT-PCR. (B) Levels of CYR61 expression in first-trimester human villous tissues from RM patients or in HCs were determined by western blotting. (C) Representative immunofluorescence images of ALKBH5 and CYR61 in frozen first-trimester villous sections obtained from RM patients and HCs. Fluorescence signals specific to anti-ALKBH5 antibodies appear green; anti-CYR61 antibodies appear red; and the DAPI-stained nuclei appear blue. (D) Global RNA m⁶A methylation level correlated positively with CYR61 mRNA levels in the villous tissue of RM patients and HCs. (E) ALKBH5 mRNA level correlated negatively with the CYR61 mRNA level in the villous tissues of RM patients and HCs.

Supplementary Material

Supplementary materials and methods, figures, and primers. <http://www.thno.org/v09p3853s1.pdf>
Supplementary table 1.
<http://www.thno.org/v09p3853s2.xls>

Acknowledgements

This work was supported by the National Natural Science Foundation of China (81401218 to F.-J.T., 81501250 to X.-C.L.), the key projects of the Shanghai Municipal Health and Family Planning Commission (201640012 to F.-J.T.), the Family Planning Project of the Shanghai Health and Family Planning Commission (20164037 to X.-C.L.), Shanghai Outstanding Young Medical Talents Training Program (X.-C.L.) and the Interdisciplinary Program of Shanghai Jiao Tong University (grant number YG2017MS38 to F.-J.T.).

Author Contributions

F.-J.T., X.-C.L., and F.J. performed most of the experiments. The molecular experiments were carried out by B.-Y.W., X.-J.Y., and W. H. The manuscript was written by F.-J.T., and X.-C.L. All the work was planned and supervised by F.-J.T. All authors have read and approved the final manuscript.

Competing Interests

The authors have declared that no competing interest exists.

References

- Wei CM, Gershowitz A, Moss B. Methylated nucleotides block 5' terminus of HeLa-cell messenger-RNA. *Cell*. 1975; 4: 379-386.
- Meyer KD, Saletore Y, Zumbo P, Elemento O, Mason CE, Jaffrey SR. Comprehensive analysis of mRNA methylation reveals enrichment in 3' UTRs and near stop codons. *Cell*. 2012; 149: 1635-1646.
- Zhang C, Chen Y, Sun B, Wang L, Yang Y, Ma D, et al. m6A modulates haematopoietic stem and progenitor cell specification. *Nature*. 2017; 549: 273-276.
- Liu J, Yue Y, Han D, Wang X, Fu Y, Zhang L, et al. A METTL3-METTL14 complex mediates mammalian nuclear RNA N6-adenosine methylation. *Nat Chem Biol*. 2014; 10: 93-105.
- Fu Y, Dominissini D, Rechavi G, He C. Gene expression regulation mediated through reversible m⁶A RNA methylation. *Nat Rev Genet*. 2014; 15: 293-306.
- Dominissini D, Moshitch-Moshkovitz S, Schwartz S, Salmon-Divon M, Ungar L, Osenberg S, et al. Topology of the human and mouse m6A RNA methylomes revealed by m6A-seq. *Nature* 2012; 485: 201-206
- Niu Y, Zhao X, Wu YS, Li MM, Wang XJ, Yang YG. N 6-methyl-adenosine (m6A) in RNA: an old modification with a novel epigenetic function. *Genomics Proteomics Bioinformatics*. 2013; 11: 8-17.
- Lee M, Kim B, Kim VN. Emerging roles of RNA modification: m6A and U-tail. *Cell* 2014; 158: 980-987.
- Zhao BS, Roundtree IA, He C. Post-transcriptional gene regulation by mRNA modifications. *Nat Rev Mol Cell Biol*. 2017; 18: 31-42.
- He C. Grand challenge commentary: RNA epigenetics? *Nat Chem Biol*. 2010; 6: 863-5.
- Meyer KD, Jaffrey SR. The dynamic epitranscriptome: N6-methyladenosine and gene expression control. *Nat Rev Mol Cell Bio*. 2014; 15: 313-326.
- Meyer KD, Jaffrey SR. Rethinking m6A Readers, Writers, and Erasers. *Annu Rev Cell Dev Biol*. 2017; 33: 319-342.
- Yang Y, Hsu PJ, Chen YS, Yang YG. Dynamic transcriptomic m6A decoration: writers, erasers, readers and functions in RNA metabolism. *Cell Res*. 2018; 28: 616-624.
- Fischer JI, Koch L, Emmerling C, Vierkotten J, Peters T, Brüning JC, et al. Inactivation of the Fto gene protects from obesity. *Nature* 2009; 458: 894-8.
- Jia G, Fu Y, Zhao X, Dai Q, Zheng G, Yang Y, et al. N6-methyladenosine in nuclear RNA is a major substrate of the obesity-associated FTO. *Nat Chem Biol*. 2011; 7: 885-7.
- Zheng G, Dahl JA, Niu Y, Fedorcsak P, Huang CM, Li CJ, et al. ALKBH5 is a mammalian RNA demethylase that impacts RNA metabolism and mouse fertility. *Mol Cell*. 2013; 49: 18-29.
- Zhang C, Samanta D, Lu H, Bullen JW, Zhang H, Chen I, et al. Hypoxia induces the breast cancer stem cell phenotype by HIF-dependent and ALKBH5-mediated m⁶A-demethylation of NANOG mRNA. *Proc Natl Acad Sci USA*. 2016; 113: E2047-56
- Zhang S, Zhao BS, Zhou A, Lin K, Zheng S, Lu Z, et al. m6A Demethylase ALKBH5 Maintains Tumorigenicity of Glioblastoma Stem-like Cells by Sustaining FOXM1 Expression and Cell Proliferation Program. *Cancer Cell*. 2017; 31: 591-606.
- Tang C, Klukovich R, Peng H, Wang Z, Yu T, Zhang Y, et al. ALKBH5-dependent m6A demethylation controls splicing and stability of long 3'-UTR mRNAs in male germ cells. *Proc Natl Acad Sci U S A*. 2018; 115: E325-E333.
- Katsube K, Sakamoto K, Tamamura Y, Yamaguchi A. Role of CCN, a vertebrate specific gene family, in development. *Dev Growth Differ*. 2009; 51: 55-67.
- Brigstock DR. The CCN family: a new stimulus package. *J Endocrinol*. 2003; 178: 169-75.
- Chen Y, Du XY. Functional properties and intracellular signaling of CCN1/Cyr61. *J Cell Biochem*. 2007; 100: 1337-45.
- Mo FE, Muntean AG, Chen CC, Stolz DB, Watkins SC, Lau LF. CYR61 (CCN1) is essential for placental development and vascular integrity. *Mol Cell Biol*. 2002; 22: 8709-8720.
- Kipkeew F, Kirsch M, Klein D, Wuelling M, Winterhager E, Gellhaus A. CCN1 (CYR61) and CCN3 (NOV) signaling drives human trophoblast cells into senescence and stimulates migration properties. *Cell Adhes Migr*. 2016; 10: 163-178.
- Gellhaus A, Schmidt M, Dunk C, Lye SJ, Winterhager E. The circulating proangiogenic factors CYR61 (CCN1) and NOV (CCN3) are significantly decreased in placentae and sera of preeclamptic patients. *Reprod Sci*. 2007; 14: 46-52.
- Tian FJ, Cheng YX, Li XC, Wang F, Qin CM, Ma XL, et al. The YY1/MMP2 axis promotes trophoblast invasion at the maternal-fetal interface. *J Pathol*. 2016; 239: 36-47.
- Graham CH, Hawley TS, Hawley RG, MacDougall JR, Kerbel RS, Khoo N, et al. Establishment and characterization of first trimester human trophoblast cells with extended lifespan. *Exp Cell Res*. 1993; 206: 204-211.
- Zhang Y, Jin F, Li XC, Shen FJ, Ma XL, Wu F, et al. The YY1-HOTAIR-MMP2 Signaling Axis Controls Trophoblast Invasion at the Maternal-Fetal Interface. *Mol Ther*. 2017; 25: 2394-2403.
- Cakmak H, Taylor HS. Implantation failure: molecular mechanisms and clinical treatment. *Hum Reprod Update* 2011; 17: 242-253.
- Zhou Y, Zeng P, Li YH, Zhang Z, Cui Q. SRAMP: prediction of mammalian N6-methyladenosine (m6A) sites based on sequence-derived features. *Nucleic Acids Res*. 2016; 44: e91.
- Raj Rai, Lesley Regan. Recurrent miscarriage. *The Lancet*. 2006; 368: 601-611.
- Pfeifer S, Fritz M, Goldberg J, McClure R, Thomas M, Widra E, et al. Practice Committee of the American Society for Reproductive Medicine Evaluation and treatment for recurrent pregnancy loss: a committee opinion. *Fertil Steril* 2012; 98: 1103-1111.
- Malassiné A, Frendo JL, Evain-Brion D. A comparison of placental development and endocrine functions between the human and mouse model. *Hum Reprod Update*. 2003; 9: 531-539
- Tsujikawa K, Koike K, Kitae K, Shinkawa A, Arima H, Suzuki T, et al. Expression and sub-cellular localization of human ABH family molecules. *J Cell Mol Med*. 2007; 11: 1105-1116.
- Kwok CT, Marshall AD, Rasko JE, Wong JJ. Genetic alterations of m6A regulators predict poorer survival in acute myeloid leukemia. *J Hematol Oncol*. 2017; 10: 39-46.
- Red-Horse K, Zhou Y, Genbacev O, Prakobphol A, Foulk R, McMaster M, et al. Trophoblast differentiation during embryo implantation and formation of the maternal-fetal interface. *J Clin Invest*. 2004; 114: 744-754
- Staun-Ram E, Shalev E. Human trophoblast function during the implantation process. *Reprod Biol Endocrinol*. 2005; 3: 56-62.
- Strickland S, Richards WG. Invasion of the trophoblasts. *Cell*. 1992; 71: 355-357.